Article:
Moontragoon, P., Vukmirovic, N., Ikonic, Z. et al. (2009) Electronic structure and optical transitions in Sn and SnGe quantum dots in a Si matrix. Microelectronics Journal, 40 (3). pp. 483-485. ISSN: 0026-2692

https://doi.org/10.1016/j.mejo.2008.06.077

Published paper
Moontragoon, P., Vukmirovic, N., Ikonic, Z. and Harrison, P. (2009) *Electronic structure and optical transitions in Sn and SnGe quantum dots in a Si matrix.* Microelectronics Journal, 40 (3). pp. 483-485.
http://dx.doi.org/10.1016/j.mejo.2008.06.077

Electronic structure and optical transitions in Sn and SnGe quantum dots in a Si matrix

P. Moontragoon, N. Vukmirović, Z. Ikonić, and P. Harrison

Institute of Microwaves and Photonics, School of Electronic and Electrical Engineering, University of Leeds, Leeds LS2 9JT, United Kingdom

Abstract

Self-assembled quantum dots in the Si-Ge-Sn system have attracted research attention as possible direct band gap materials, compatible with Si-based technology, with potential applications in optoelectronics. In this work, the electronic structure near the Γ-point and the interband optical matrix elements of strained Sn and SnGe quantum dots in a Si matrix are calculated using the eight-band **k.p** method, and the competing L-valley conduction band states were found by the effective mass method. The strain distribution in the dots was found within the continuum mechanical model. The bulk band-structure parameters, required for the **k.p** or effective mass calculation for Sn were extracted by fitting to the energy band structure calculated by the non-local empirical pseudopotential method (EPM). The calculations show that the self-assembled Sn/Si dots, with sizes between 4 nm and 12 nm, have indirect interband transition energies (from the size-quantized valence band states at Γ to the conduction band states at L) between 0.8 to 0.4 eV, and direct interband transitions between 2.5 to 2.0 eV, which agrees very well with experimental results. Similar good agreement with experiment was also found for the recently grown SnGe dots on Si substrate, covered by SiO_2. However, neither of these are predicted to be direct band gap materials, in contrast to some earlier expectations.

1. Introduction

The Si-Ge-Sn alloys are considered as an interesting material for future optoelectronic semiconductor devices, compatible with Si technology [1]. Control of their properties can be achieved by varying the alloy composition, as found in experimental and theoretical investigations [2-8], indicating their potential for optoelectronic applications. Self-assembled Sn quantum dots embedded in Si have been successfully grown, and it was anticipated that these would be important, direct-gap nanostructures for optoelectronic devices, a property not found in the more conventional SiGe quantum dots. Although bulk Sn is a direct zero band gap semiconductor, the gap at the Γ-point is expected to increase, as a combined result of quantum confinement and strain. The Sn/Si dots were grown by temperature modulated molecular beam epitaxy. A few nanometers thick epitaxially-stabilized metastable Sn_xSi_{1-x} alloy layer with x=0.05-0.1 was first grown on Si (001), and then annealed at temperatures between 550 and 800^o C. The process is based on a very small equilibrium solubility of Sn in Si, which leads to clusterization of Sn atoms upon annealing the metastable alloy, leaving behind more or less pure Si. The luminescence measurements [9] show a relatively weak broad spectrum at 0.7-1 eV. Similarly, SnGe alloy dots have recently been grown on Si. Theoretical studies of the electronic structure of Sn-based quantum dots, which should help in understanding the features observed in experiments, are missing. In this work, we therefore calculate the electronic structure and interband absorption in this type of dots within the framework of envelope function theory. Due to lack of some of material parameters for Sn, these were extracted from calculations using the empirical nonlocal pseudopotential method.

2. Computational method

Due to a large difference of Si and Sn lattice constants the dots are strained, and this was described within the continuum mechanical model and calculated by the finite element method. The Γ-valley electronic structure and interband optical matrix elements were calculated using the eight-band **k.p** method with strain [10]. Details of the quantum dot electronic structure calculation are given in [11]. This requires a number of parameters, which are well tabulated for Si and Ge (e.g. [12]), while the data for Sn are more scarce or completely missing, so we have extracted all the relevant parameters from empirical nonlocal pseudopotential calculations. For this purpose we started with the set of formfactors given in [13], and devised a continuous formfunction for Sn, which reproduces very well the known band structure features [14,15], and finally used it to extract the parameters for relaxed and strained conditions. The obtained values are: the Luttinger parameters γ_1=-25.19, γ_2=-15.11, γ_3=-13.53, Kane energy E_p=14.26 eV, the conduction band parameter A'=-3.25, c.b. hydrostatic deformation potential a_c=-8.714 eV, v.b. hydrostatic, uniaxial, and shear deformation potentials a_v=1.62 eV, b=-2.01 eV, d=-0.39 eV, spin-orbit splitting Δ=0.70 eV, direct band gap E_g=-0.408 eV. These parameters were used in the 8-band **k.p** calculation for quantum dots.

The L-valley size-quantized states of Sn dots are calculated by the effective mass method, using the scalar, angle-averaged effective mass of the ellipsoidal L valleys, and

accounting for the hydrostatic strain only. As for the L-valley parameters, the longitudinal (m_l) and transverse (m_t) effective mass are found to be 1.99 and 0.091, respectively, in good agreement with other published values [14], and a value of -2.24 eV was extracted for the L valley hydrostatic deformation potential.

The valence band offset at the $Sn/Si_xGe_ySn_{1-x-y}$ interface was taken in accordance to [16], i.e. $\Delta V_{v.b.}=1.17x+0.69y$ [eV].

3. Results and discussion

Using the methods and material parameters described above we have investigated the electronic and optical properties of the Sn-based quantum dots, in particular Sn quantum dots embedded in Si and the $Ge_{1-x}Sn_x$ alloy dots.

The electronic structure of Sn dots in Si was calculated assuming they were either cylindrical, lens or cone shaped, and since the results for the three are not too different we here show only those for cylindrical dots. The calculated strain distribution is displayed in Fig.1. The Sn/Si interface has type-I band alignment, i.e. the Sn dot is the potential well for both electrons and holes at the Γ point. The direct-transition absorption spectrum of a couple of dot sizes is shown in Fig.2. As expected, the transition energy inversely depends on the dot size. The main feature is that the direct absorption spectrum of Sn/Si dots peaks around 2-2.5 eV. This is larger than the indirect absorption onset in bulk Si (matrix), at about 1.1 eV, but since this latter absorption is relatively weak one can still expect that these direct transitions might be observed in very thin layers of Si containing Sn dots. It is quite a surprising result that the direct transition energies are so large. This is because of the very large strain in Sn, so large, in fact, that the zero-gap material has become an almost wide-bandgap semiconductor.

However, calculation of L-valley quantized states (the band alignment is here also type-I) shows that these states are much lower in energy than the conduction band states at Γ, as shown in Fig.3, hence the Sn/Si quantum dots are not a direct gap material. This is a consequence of the fact that the absolute value of L-valley hydrostatic deformation potential is much smaller than that of the Γ valley. Therefore, the effects of strain change the arrangement of Γ and L-valley states. The photoluminescence peak at approx. 0.7 eV, observed in [9] in Sn dots with the diameter of about 5 nm, agrees very well with the indirect transition energy predicted here, so we believe that it is actually this (indirect and weak) transition that was observed. The likely mechanism for this was the photogeneration of electrons in the X valley of the Si matrix, followed by their capture into lower lying L states of Sn dots, and then by the indirect, phonon-assisted recombination.

Previous studies of Si-Ge-Sn bulk alloys [2-8] show that a direct gap material can be obtained in a suitable range of $Ge_{1-x}Sn_x$ alloy compositions, so we have also calculated the electronic structure of $Ge_{1-x}Sn_x$ dots embedded in Si. Clearly, such dots cannot be grown in Si in the same way as Sn dots are, because Ge is completely soluble in Si, in

contrast to Sn. However, growth of $Ge_{1-x}Sn_x$ dots on [111] oriented Si substrate, rather than in a Si matrix, has been recently reported [17]. The dots are approximately hemispherical in shape, they are covered by SiO_2, and are asserted to have a coherent interface with the underlying Si, and are therefore strained. It is less clear, however, what strain conditions apply towards the `upper' interface with SiO_2, since it even has a different crystalline structure. Furthermore, the different crystalline structures of Sn and SiO_2 would discourage one to use the **k.p** method at all, but the large band discontinuities between Sn and SiO_2 effectively make it irrelevant what is on the other side of Sn, and the **k.p** method can still be used to good accuracy. Overall, we expect that the calculation for $Ge_{1-x}Sn_x$ dots fully embedded in Si, with their axis in the [001] direction, as was performed in this work, is an approximate description of the actual structure.

In these calculations the Luttinger parameters, deformation potentials and the spin-orbit splitting of $Ge_{1-x}Sn_x$ were estimated using Vegard's law, while the direct band gap and lattice constant were calculated by using the quadratic interpolation, with bowing parameters of 2.49 eV [2.4.18] and 0.0166 nm [19], respectively. The results for the dot sizes between 4 and 12 nm, and for different compositions $0<x<1$, show that indirect interband transitions (towards the L valley states) occur from 0.8 to 0.4 eV, while the direct interband transitions occur from 2.5 to 1.5 eV, as shown in Fig.3, implying that these dots are indirect gap materials. The direct energy band gap depends quadratically on the Sn composition (note the non-monotonic dependence of E_g on x in Fig.3), because the bowing parameter in the direct band gap of the alloy has a strong influence. Experimentally, for dots of small diameters (<10 nm) absorption peaks between 1.5 eV and 2 eV were found [17], which agrees very well (perhaps surprisingly so, in view of the approximations involved) with the data for direct transitions given in Fig.3. Nevertheless, these dots are (predicted to be) an indirect band gap material.

4. Conclusion

Using the 8-band **k.p** and the effective mass method, we have explored the properties of self-assembled Sn and $Ge_{1-x}Sn_x$ quantum dots in Si. The self-assembled Sn/Si dots of size between 4 nm and 12 nm were found to have indirect interband transitions (towards the L-valley size-quantized states) from 0.8 to 0.4 eV, and direct interband transitions from 2.5 to 2.0 eV, which compares very well with the experiments. However, the indirect nature of the lowest interband transition makes Sn or SnGe quantum dots in a Si matrix the unlikely candidates for optoelectronic devices, except perhaps for pure absorption applications, in contrast to some previous expectations.

References:

[1] G. Sun, H. H. Cheng, J. Menendez, J. B. Khurgin, and R. A. Soref, Appl. Phys. Lett. 1990; 90: 11992-11994.
[2] G. He, and H. A. Atwater, Phys. Rev. Lett. 1997; 79: 1937-1940.
[3] M. Bauer, J. Taraci, J. Tolle, A. V. G. Chizmeshya, S. Zollner, D. J. Smith, J. Menendez, C. Hu, and J. Kouvetakis, Appl. Phys. Lett. 2002; 81: 2992-2994.
[4] P. Moontragoon, Z. Ikonić, and P. Harrison, Semicond. Sci. Technol. 2007; 22: 742-748.
[5] J. Kouvetakis, J. Menendez, and A. G. V. Chizmeshya, Annual Review of Materials Research 2006; 36: 497-554.
[6] J. Kouvetakis, and A. G. V. Chizmeshya, J. Mater. Chem. 2007; 17: 1649-1655.
[7] Y. Lei, P. Mock, T. Topuria, N. D. Browning, R. Ragan, K. S. Min, and H. A. Atwater, Appl. Phys. Lett. 2003; 82: 4262-4264.
[8] R. Ragan, K. S. Min, and H. A. Atwater, Materials Science and Engineering B 2001; 87: 204-213.
[9] A. Karim, G. V. Hansson, W.-X. Ni, P.O. Holtz, M. Larsson, and H. A. Atwater, Optical Materials 2005; 27: 836-840.
[10] T. B. Bahder, Phys. Rev. B 1990; 41: 11992-12001.
[11] N. Vukmirović, Z. Gačević, Z. Ikonić, D. Indjin, P. Harrison, and V. Milanović, Semicond. Sci. Technol. 2006; 21: 1098-1104.
[12] S. Ridene, K. Boujdaria, H. Bouchriha, and G. Fishman, Phys. Rev. B 2001; 64: 085329-9.
[13] J. R. Chelikowsky, and M. L. Cohen, Phys. Rev. B 1976; 14: 556-582.
[14] T. Brudevoll, D. S. Citrin, M. Cardona, and N. E. Cristensen, Phys. Rev. B 1993; 48: 8629-8635.
[15] S. Adachi, J. Appl. Phys. 1989; 66: 813-819.
[16] M. Jaros, Phys. Rev. B 1988; 37: 7112-7114.
[17] Y. Nakamura, A. Masada, and M. Ichikawa, Appl. Phys. Lett. 2007; 91: 013109-3.
[18] V. R. D'Costa, C. S. Cook, A. G. Birdwell, C. L. Littler, M. Canonico, S. Zollner, J. Kouvetakis, and J. Menendez, Phys. Rev. B 2006; 73: 125207-6.
[19] P. Aella, C. Cook, J. Tolle, S. Zollner, A. V. G. Chizmeshya, and J. Kouvetakis, Appl. Phys. Lett. 2004; 84: 888-890.

FIGURE CAPTIONS

Fig.1. Strain distribution in cylindrical Sn quantum dots in Si matrix.

Fig.2. The direct interband absorbtion spectra of cylindrical Sn/Si quantum dots for different dot diameters d. Solid lines correspond to z-polarized light (along the dot axis), and dashed lines to in-plane polarized light.

Fig.3. The dependence of the band gap of $Ge_{1-x}Sn_x/Si$ dots on the diameter and composition x.

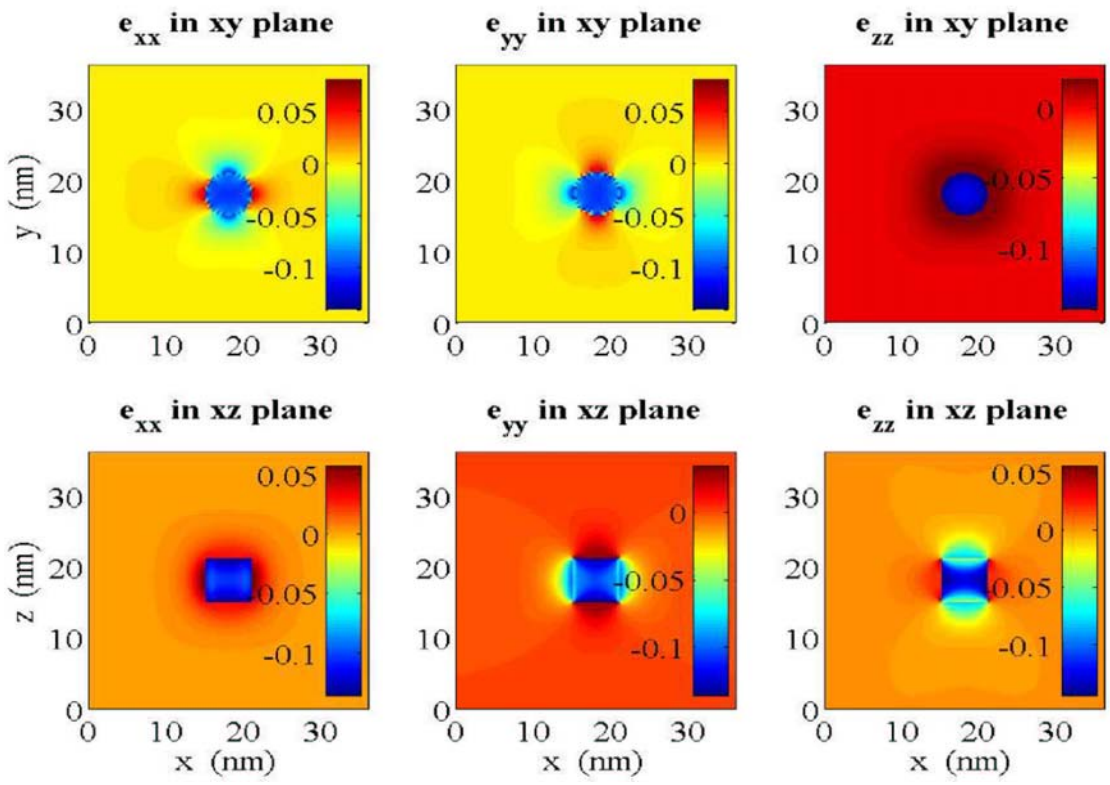
e_xx in xy plane
e_yy in xy plane
e_zz in xy plane
e_xx in xz plane
e_yy in xz plane
e_zz in xz plane
y (nm)
z (nm)
x (nm)
0.05
0
-0.05
-0.1
0
10
20
30

Fig.1

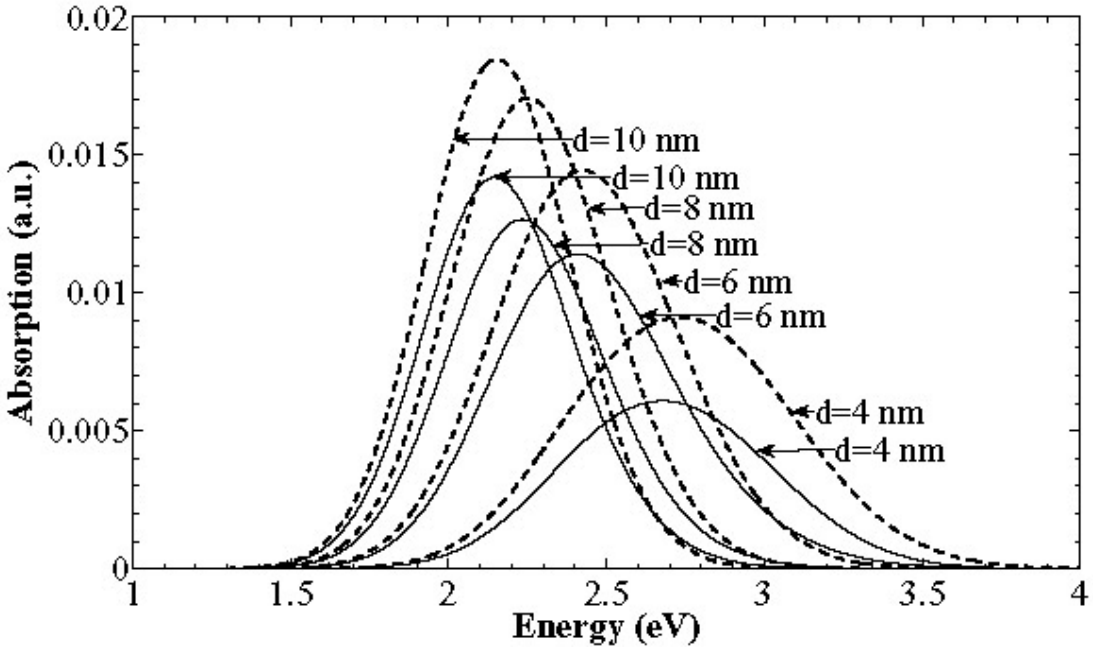
0.02
0.015
0.01
0.005
0
Absorption (a.u.)
1
1.5
2
2.5
3
3.5
4
Energy (eV)
d=10 nm
d=10 nm
d=8 nm
d=8 nm
d=6 nm
d=6 nm
d=4 nm
d=4 nm

Fig.2

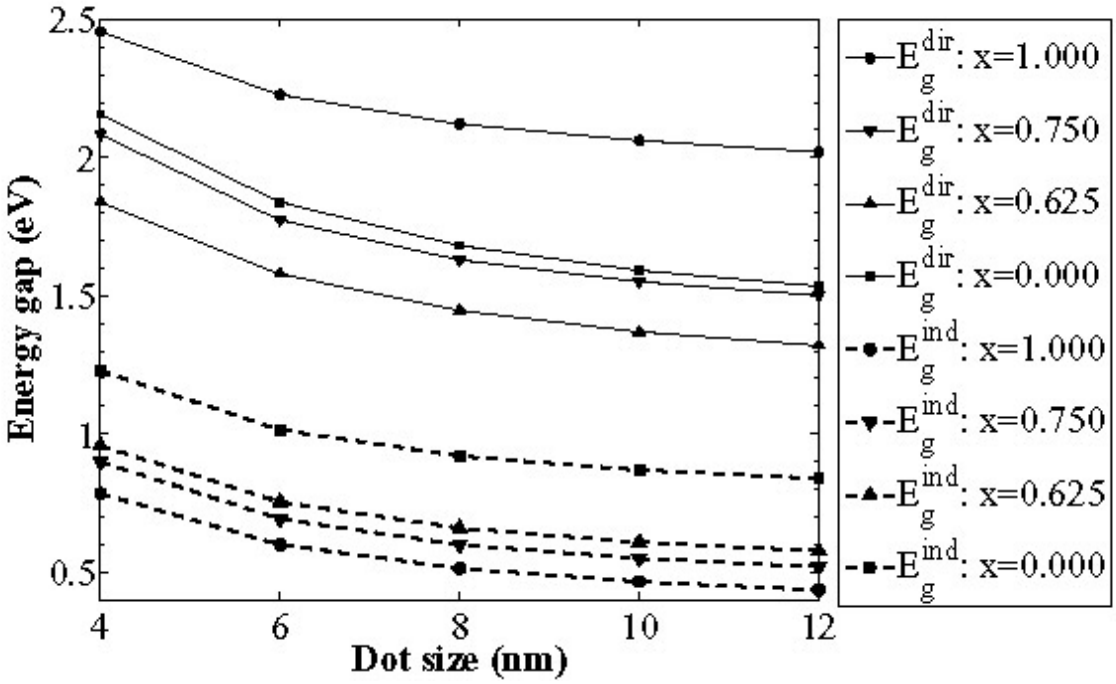
2.5
2
1.5
1
0.5
Energy gap (eV)
4
6
8
10
12
Dot size (nm)
E_g^{dir}: x=1.000
E_g^{dir}: x=0.750
E_g^{dir}: x=0.625
E_g^{dir}: x=0.000
E_g^{ind}: x=1.000
E_g^{ind}: x=0.750
E_g^{ind}: x=0.625
E_g^{ind}: x=0.000

Fig.3